Engineering Failure Analysis 133 (2022) 105950

Contents lists available at ScienceDirect

Engineering Failure Analysis

journal homepage: www.elsevier.com/locate/engfailanal

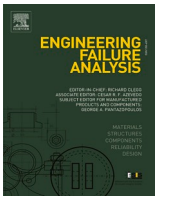

Analysis of the failure and remedial measures taken after the collapse of a historical bell

Salvador Ivorra [a,*], Benjamín Torres [a], Alfonso C. Cárcel [b]

[a] Civil Engineering Department, Universidad de Alicante, Spain
[b] Mechanical and Materials Engineering Department, Universiat Politècncia de València, Spain

ARTICLE INFO

Keywords:
Bell
Fatigue failure
Failure analysis
Remedial measures
Cyclic loading
Forensic engineering

ABSTRACT

This paper describes the collapse analysis of the historical *El Jaume* bell, cast in 1429, one of the bells in the Cathedral of Valencia's *Micalet* bell tower (Spain). In 1992 the yoke was completely restored and given a new steel axis. The failure occurred when the bells were being rung on Christmas Day 2014, fortunately without any casualties. After several field visits to assess the damage and failure "in situ", a diagnosis was made of the causes of the failure. The diagnosis was the result of (1) a detailed visual inspection, (2) a metallographic and fractographic analysis of the fractured steel axis, (3) a fatigue damage analysis by finite element modelling software and (4) an estimation of the bell's remaining fatigue life cycle using Whöler S-N curves. In view of the results obtained it was concluded that the fatigue life cycle should have been reached between 300,000 and 400,000 cycles, while the failure occurred at 346,500 cycles. Although these elements are usually designed to not fail during its life, they can sometimes suffer cracks during cyclic ringing. One of the main causes of the fatigue failure was the incorrect design of the steel gudgeon, which produced a high stress concentration and drastically reduced the fatigue strength at 10^6 cycles. The paper also describes the remedial measures taken to avoid fatigue failure in the other bells and the lessons that have been learned from the experience.

1. Introduction

From earliest times to the present day bells have been used to announce events and have marked the life of villages. The bells' primordial mission has always been to inform (also to coordinate, mark out territory and even at times to protect [1]), fundamentally to call the faithful to church services and tell the time from morning to night. So that the bells could be heard at a considerable distance, the church steeples always towered above the roofs of the surrounding houses and had gaps in their walls to give the sound waves a free passage [2]. Throughout history bell ringing has been done manually by ropes to swing the bell partially or completely around its axis.

In the 1950s changes began to be made to the traditional ways of life in Spain and the ringing of the bells changed to an electrically-powered system [1]. This was based on either a clapper hitting the motionless bell or a system that swung the bell itself. However, at the end of the 80s unpaid bell-ringing volunteers began to appear who not only operated the bells manually but recovered the old traditional chimes, undertook renovations and publicized their activities [3]. Bell ringing is now a deeply rooted tradition. Manual bell ringing is based on rhythms and is used almost everywhere for religious festivals. The technique consists of a team of bell-ringers making a set of bells chime together simultaneously to create a musical effect.

* Corresponding author.
E-mail address: sivorra@ua.es (S. Ivorra).

https://doi.org/10.1016/j.engfailanal.2021.105950
Received 21 August 2021; Received in revised form 25 November 2021; Accepted 30 November 2021
Available online 4 December 2021

There are three types of bell ringing systems [4]: Central European, English and Spanish. The English and Spanish systems swing the bell completely round its axis, the bells are directly anchored on the tower windows and rotate continuously in the same direction, while in central Europe the bells tilt on their axis at an angle that varies from the vertical to between 50° and 160° [4,5]. The difference between the English and Spanish systems is that the English is highly unbalanced and changes the direction of the swing in each cycle, while in the Spanish a counterweight provides a high level of balance and the bell always turns in the same direction.

All the bell-ringing systems generate a dynamic interaction problem with the structure of the supporting bell tower due to the inertial forces generated by the movement of the bells. In the English and central European systems this dynamic interaction, the damage caused and the reinforcements applied [6] have been studied in depth [5,7,8,9,10,11,12,13,14,15], but have received less attention in the Spanish systems [4,5,16]. During a period of years or even centuries, the daily ringing of the bells submits the bell gudgeons and anchorages to cyclic loads. Although these elements are designed to not fail during its life, they occasionally get damaged due to the crack propagation caused by cyclic forces [17,18]. The fatigue cracks originate in microstructures and reduce the fatigue lifecycle of high strength steels, so that more and more attention has been paid to research on how fatigue cracks are initiated [19,20]. Failure and collapse of a bell, although it is unusual (the authors of this article have only identified two scientific publications in which it is explained in depth the failures that occurred in the Freedom Bell, [21], Liberty Bell [22] and Big Ben Bell [22]), its consequences can be very serious, since:

- This occurs in an element of considerable size and weight that turns around its axis at various revolutions per minute.
- Manual operations imply the presence of bell ringers close to the bell.
- To allow the sound waves a free passage outside, the bell is in front of an open space in the wall and in case of failure could easily be hurled out of the tower itself.

A study in [21] describes the failure of the Freedom Bell in Berlin: the clapper hanging broke in 1966 and the clapper itself broke in 1979, both by fatigue fractures [21]. Cyclical movements generate vibratory phenomena that can compromise structural safety and reduce the effective lifecycle [23] and frequently damage the axis, bearings and supporting structure. Other studies [22] have used a simple model based on energy methods of applied mechanics to study the effect of clapper location on the initiation and growth of cracks in bells. This model analysed the origin of cracks in the Liberty Bell in Philadelphia and Big Ben in London, and the simple model has been used to explain why remedial measures on Big Ben, though perhaps not optimal, have prolonged its lifecycle [22]. The great St. Peter's Bell in Cologne Cathedral is another well-known case. The clapper and its mounting were removed in April 2017 after it was discovered that repair work in the fifties had left the clapper striking the bell in the wrong place and so causing material damage to the bell.

Apart from the two above-cited cases [21,22], no other papers have been found on the collapse of bells and other problems associated with fatigue of bells [21,22]. Within this general context, this paper describes the failure of the bronze *El Jaume* bell with a total weight 28.5 kN (17.5 kN of bronze plus an 11 kN counterweight) that occurred in Valencia Cathedral when the bells were being rung on Christmas Day 2014. The paper is organized as follows: Section 2 contains a general description of the building, the *El Jaume*

Fig. 1. (a)- *El Micalet* bell tower. (b)- Bell ringers ringing the bell manually (c)- *El Jaume* bell.

bell and the bell-ringing system. Section 3 describes the investigation and visual inspection carried out after the failure of the bell to assign the causes. Section 4 explains the metallographic and fractographic analyses of the cylindrical shaft after the collapse. Sections 5, 6 and 7 contain a fatigue damage analysis by finite element modelling and quantitative analysis of the damage based on Whöler fatigue curves [24], SN (Stress-Number of cycle) and formulates a definitive diagnosis. Section 8 describes the repairs, improvements and remedial measures carried out to avoid the repetition of the problem, while our conclusions and the lessons learnt from the experience are given in Section 9.

2. EL Jaume bell in the micalet bell tower

The Cathedral of Valencia and its bell tower *El Micalet*, in the city's historical centre, is thought to have been constructed around 1270 in the Valencian Gothic style. The octagonal tower, named Micalet, was built between 1381 and 1429, is 63 m high and has a 51 m perimeter (Fig. 1a).

The first floor is solid stone apart from the central staircase. The second floor is vaulted with a single window to the outside, the third is larger and similarly constructed with two windows, and the belfry on the top floor with eight windows, seven of which are occupied by bells.

There are 11 bells in the bell room (*Catalina, Violante, Úrsula, Bárbara, Pablo, Narciso, Vicente, Andrés, Manuel, Jaume* and *María*) [25], all of which are rung manually (Fig. 1b) by ropes [24]. Bárbara has an electric motor installed for daily chimes only. The three oldest (*Catalina, El Jaume* and *Pablo*, which date from 1305, 1429 and 1489) were shown at the Seville International Exposition in 1992, when they were declared part of the National Heritage [27]. For the International Exposition the bells were restored and the bearings were replaced due to the accumulation of fatigue damage.

On Christmas Day 2014 *El Jaume* bell (Fig. 1c) suddenly collapsed when being rung manually. Due to the bell's famous reputation the news was reported in the national and international media.

This bell weighs approximately 28.5 kN including counterweight, fittings, bronze bell and clapper, an estimate confirmed by historical documents and obtained by Eq. (1) [28,29]:

$$W(kN) = 1.6 \bullet 5.79 \bullet D^3 \tag{1}$$

where W (kN) is the weight of the counterweight, fittings, bell and clapper and D is the diameter of the bell mouth. From its restoration in 1992 until its collapse in 2014 the bell was rung approximately 30 times each year for 15 min at around 35 revolutions per minute [28].

3. Investigation of the failure

After the failure the bell fell 4 m to the belfry floor, fortunately without causing any injuries. In the first visual inspection (Fig. 2) it was seen that:

Fig. 2. Photos taken after the collapse of the bell.

- The bell canons, which join the bell to its counterweight, were completely fractured (Fig. 2a and b).
- The circular gudgeon left the support. The left-hand bearing anchorage suffered no apparent damage (Fig. 2c).
- The bell's left-hand steel shaft gudgeon was also broken (Fig. 2d-e).
- The right-hand bearing anchorage was split (Fig. 2f).
- The bell's right-hand steel shaft gudgeon was out of his position but not broken.

The bright colour of the cross-section of the five broken canons without signs of oxidation or to the sudden application of higher stresses than they could resist. The bell was in a vertical position on the floor, indicating that the fracture occurred with the bell horizontal to the outer tower wall.

The axis is formed by a large wooden counterweight and a weight of approximately 11 kN. The lower bronze surface is anchored to this element by metal braces connected to the canons (Fig. 1b). In the zone close to the supports with the structure the wooden counterweight has a prismatic groove 650 mm long with two cross sections: the first is 550 mm long with a square 60x60 mm cross-section anchored to the counterweight with bolts and clamps, the second has a circular 55 mm diameter cross-section 100 mm long that protrudes from the counterweight inserted into the bearing anchorage and allows the axis to swing freely.

The fracture of the bell's left-hand steel shaft gudgeon occurred just where the square section joined the circular section (Fig. 2d and e). The fact that there is no gradual transition between the square and circular sections is of special importance as this creates a zone with high stress concentration. The visual inspection of the fracture (Fig. 3) revealed four clearly different circular zones (A, B, C and D). The centres of the first three zones are out with respect to the geometric center of the steel axis while D is concentric with the axis. A section is approximately circular, rough and was the ultimate section to resist stresses so that the final break was ductile once the cross section was yielded by overload. B is less rough than A and is due to the cyclical tension-compression stresses on the axis, and moved upwards due to most of the cracks being on the underside of the gudgeon. Zone C was reddish due to oxidation, indicating that it had been open to the atmosphere for some time. D was brightly coloured and smooth due to the friction between the two sides of a crack and this was where the fracture of the axis began.

According to [30], this type of failure is typical of a shaft subjected to tension-compression stresses derived from positive-negative bending under low stresses – the bell goes through relatively few revolutions compared to an industrial machinery - but with severe stress concentrations (Fig. 4). Presence of ratchets is another characteristic feature of fatigue failures in rotating bending shafts (Fig. 3).

Finally, Fig. 2c and f show the steel shaft gudgeon supports: in Fig. 2c it can be seen that the circular gudgeon left the support – which suffered no apparent damage – after the break, while 2f shows the destroyed right gudgeon support.

From the above evidence it can be said that the collapse took place in the following phases: 1) fracture of the left-hand gudgeon when the bell was practically horizontal to the outer wall, probably due to a fatigue crack initiated in the transition of the circular-to-square section; 2) when the gudgeon broke it was forced out of the right-hand support and the weight of the bell together with its inertial forces caused the fracture of the bearing anchorages; and 3) the bronze and the counterweight fell to the floor at an angle no greater than 50° causing the brittle fracture of the canons. The bell itself remained mouth-down and the counterweight fell beside it.

4. Metallographic and fractographic analysis

The external broken part of the steel shaft gudgeon was submitted to a metallurgic analysis to determine the type of steel, its condition and mechanical properties. An 8 mm thick cross-section sample was taken from the end of the shaft by abrasive cutting under strong refrigeration, polished and etched to perform a metallographic analysis. Hardness was measured on polished sections using

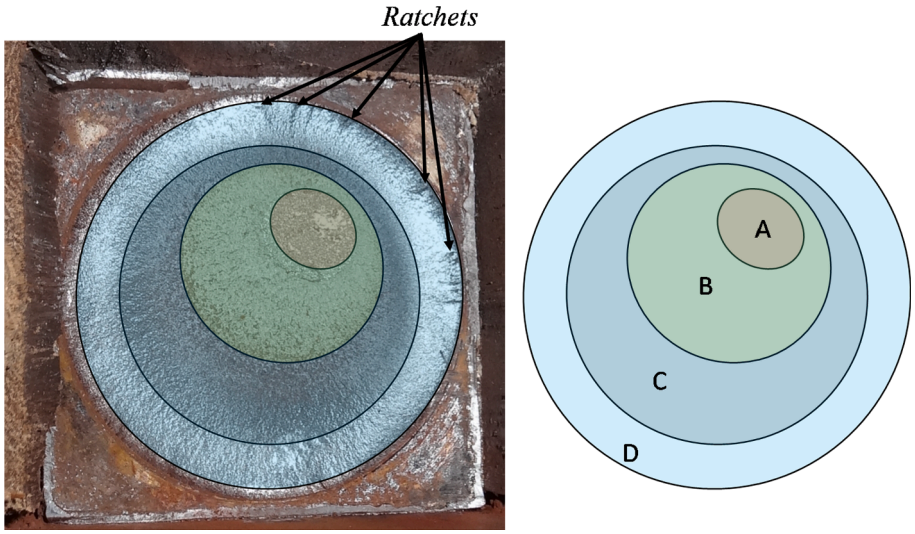

Fig. 3. Cross section of the different zones of the fractured axis.

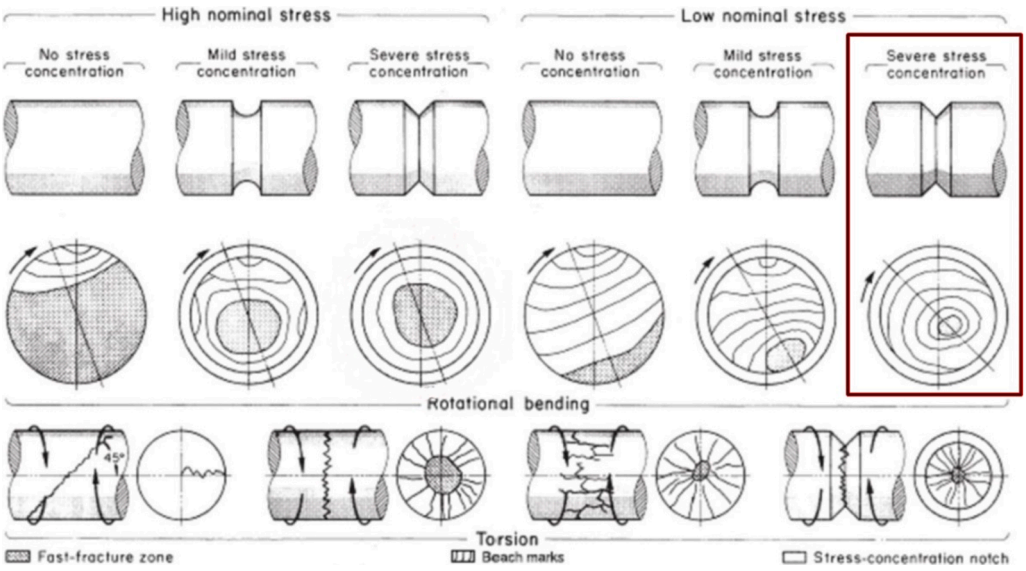

Fig. 4. Schematics of fatigue fracture surfaces from ASM Metals Handbook [30]. Obtained from [31].

Rockwell HRB tests. The equivalent ultimate strength of the steel was estimated from the values of HRB hardness using the equivalence determination methods included in DIN 50,150 and EN-ISO 18,265 standards [32]. (HRB values were used for estimation of ultimate strength because they were more reproducible than HB measures). In addition, tensile mechanical tests were performed.

Table 1 gives the results of HRB hardness tests and the equivalent values of ultimate strength R_m or S_u, including the uncertainty of the predicted values, as obtained from the appropriated conversion tables included in the standards.

Tensile mechanical strength of the steel at ambient temperature was measured in tensile tests as per EN-ISO-6892 [33] standard, using an Instron 4204 test rig at strain rate values of 0.4 min^{-1}. Three longitudinal tensile specimens (of section 25 mm^2 and total length 75 mm) were extracted by refrigerated cutting and machining from a section at 50% of the gudgeon radius from the surface, as required by EN-ISO 377 [34]. (Tensile strength was also estimated in a preliminary study from hardness HRb values, and then converted to tensile strength Rm values as per EN-ISO 18,265 standard [35]). Table 2 shows the values of mechanical properties measured and, for reference purposes, the values required for grade C45, C50 and C55 non alloyed steels from EN-ISO 683 [36] after a normalizing heat treatment.

Fig. 5 shows the sample microstructure as observed in an optic Nikon Microphot microscope after polishing and etching with Nital3 reagent. It consists of proeutectoid ferrite (creamy color grains) and pearlite grains (brown grains).

The average microstrutural grain size is very fine. The intercepted length by each grain ranges between 0.018 mm and 0.030 mm, which corresponds to a normalized grain size of index $G = 7 \sim 8$ according to the standard measurement method EN-ISO 643: Steels. Micrographic determination of the apparent grain size [37].

This fine grain size and the ferritic-pearlitic microstructure is typical of medium carbon 0.40–0.50% C hypo eutectoid steels in a normalized condition or heat treatment. The exact type of steel is unknown, but both microstructure and properties observed are similar to those corresponding to the widely used and well-known non alloyed C40 or C45 construction steels [38]. Table 3 gives the composition and properties of these steels.

A fractographic visual inspection near the fracture section of the steel shaft gudgeon was carried out using a Nikon stereoscopic microscope. Some surface irregularities that could act as crack initiation sites can be seen in Fig. 6 (fracture section on the left of the image). These indentation marks were probably caused by the tool used to insert and fix the gudgeon into the wooden counterweight. The fine surface and parallel line marks due to machining can be observed on the right side of the images.

5. Numerical approach for fatigue damage

After the visual investigation of the collapse, metallographic and fractographic analysis of the steel gudgeon it seems to indicate that a fatigue failure had occurred in the transition from square to circular section. With the aim of approaching the cause that has originated the collapse, a finite element numerical model (FEM) of steel gudgeon has been carried out. It is a static model of the steel

Table 1
Results of hardness test and equivalent values of Rm.

Hardness Test	Min	Max	Average	Reproducibility %	Equivalent Rm (MPa)	Uncertainty (MPa)
HRB	95	96	95.67	2.91	745	±20

Table 2
Mechanical properties of the steel.

Material	Specimen	Proof strength Rp0.2 (MPa)	Tensile strength Rm (MPa)	A%	Hardness HRb	Rm from hardness measurements EN-ISO 18,265 (MPa)
Bell shaft	1	438	745	12.5		
	2	382	720	17.8		
	3	372	714	14.9		
	Average	397.3	726.3	15.1	95.67	745 ± 20
Minimum values EN ISO 683						
C45 steel		340	620	14		
C50 steel		355	650	12		
C55 steel		370	680	11		

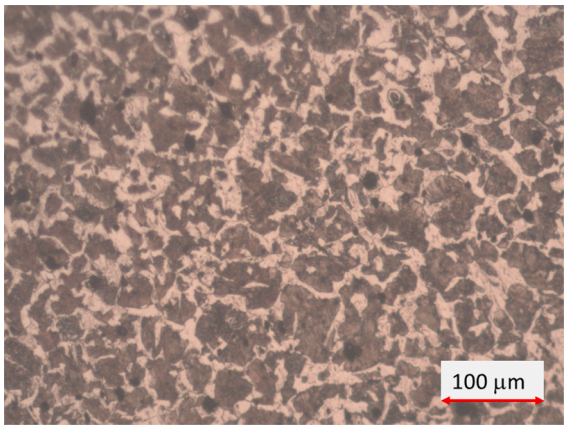

Fig. 5. Microestructure of the gudgeon steel after polishing and etching with Nital 3. 100X.

Table 3
Composition and properties of C40 and C45 steels (EN10083-2; ISO 683–1 [38,36]).

Type	Document	% Composition					
		C	Mn	Si	P	S	Ultimate Strength (MPa) Heat treatment + N
C40	EN-ISO 683-1 EN 10083-2	0.37–0.44	0.5–0.8	0.1–0.4	<0.035	<0.035	> 580
C45		0.42–0.50	0.5–0.8	0.1–0.4	<0.035	<0.035	>620

gudgeon, which the loading corresponding to inertial forces caused by the bell swinging have been applied. A fatigue analysis has been performed to identify the stress concentration section, the evolution of fatigue damage and the lifecycle in which the failure occurs.

The numerical study was carried out with Lusas software [39]. Steel gudgeon was modelled with hexahedra 3D HX20 solid elements (Fig. 7a). Each of these elements had 20 nodes, each node with three degrees of freedom (Translation along X, Y, Z). For material properties, a conventional steel has been used with a Youngś Modulus of 210000 MPa, a Poissońs ratio of 0.3 and a mass density of 7.8 $\cdot 10^{-9}$N/mm^3. All the model elements had linear elastic behaviour. The model (Fig. 7b) has a total number of 1344 finite elements.

Fatigue calculations can be performed on the results of a linear finite element stress analysis using the total life approach. The fatigue life may be expressed in terms of the damage that is done to the gudgeon by a prescribed loading sequence or as the number of repeats of the sequence that will cause failure of the structure. In fatigue analysis, a measure of damage D is obtained using Mineŕs rule [40], that is:

$$\text{Damage } D = \frac{n_1}{N_1} + \frac{n_2}{N_2} + \cdots \frac{n_i}{N_i} \tag{2}$$

Where:

- D is the damage variable, a factor representing that the damage the material has sustained due to the applied loading and number of cycles. A value>1 indicates failure.
- n_i is the number of cycles of stress applied to the structure.
- N_i is the life corresponding to the stress.

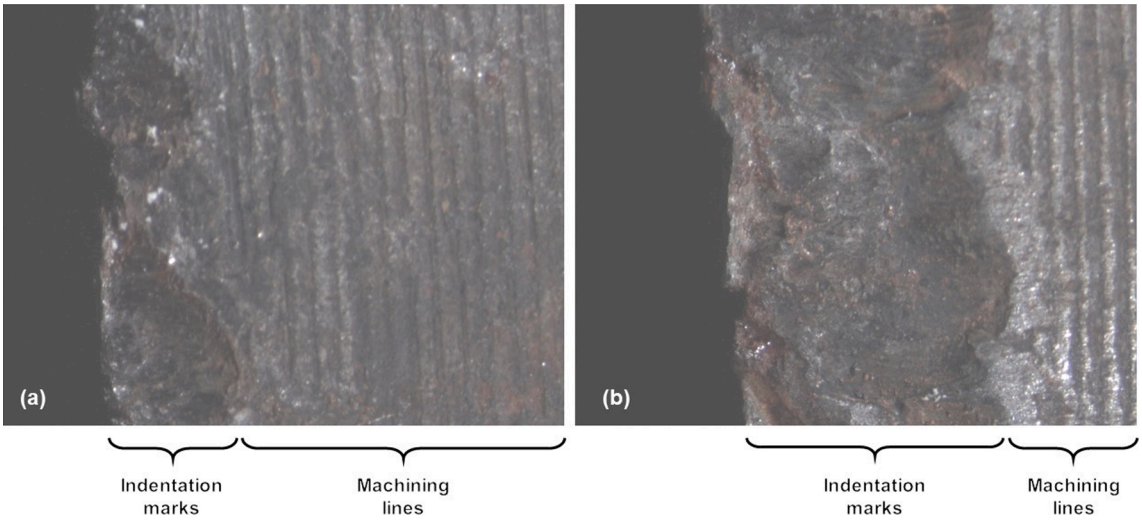

Fig. 6. Stereoscopic images of the gudgeon surface immediate to the fatigue fracture. (a) 10X, (b) 50X.

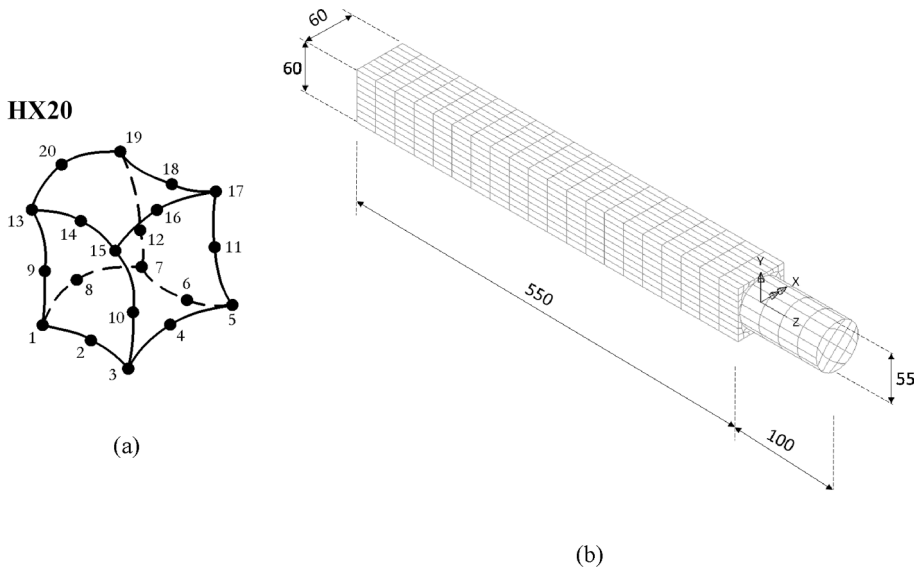

Fig. 7. (a)- Hexaedra 3D HX20 element. (b)- Finite element model of the steel axis (mm).

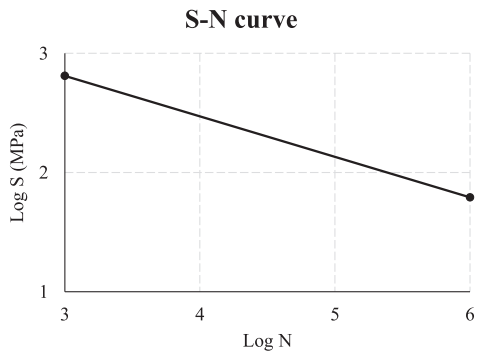

Fig. 8. S-N curve used in a numerical fatigue simulation.

To carry out fatigue analysis using Lusas [39], service conditions and material properties must be defined, i.e. a S-N curve (stress-number of cycles) and fatigue loading spectrum. The fatigue loading spectrum defines the loading sequence in terms of the number of cycles of each load case that are to be applied to the structure. To obtain an estimate of the number of cycles that cause a damage value of 1, the fatigue loading spectrum will be varied until identifying the areas in which the damage value is equal to 1. The SN curve contain the variation in stress values with the number of cycles to failure and are defined on a Log-Log scale. Fig. 8 shows the SN curve used in this analysis. The procedure to obtain it, will be detailed in the following section.

Fig. 9 shows a 3D plot of the damage distribution along the steel gudgeon for numbers of cycles corresponding to 300,000 (Fig. 3a) and 400,000 (Fig. 3b) cycles. In view of the results, it is observed that fatigue damage is concentrated and accumulated in the perimeter of circular section transition to square section. Around 300,000 cycles starts the fatigue damage, with damage values of $D = 1.06$ in certain small areas of the perimeter. For a value of 400,000 cycles, damage has spread along the perimeter, extending the damage zone and reaching most of the perimeter.

Fig. 10 shows the fatigue damage value and propagation in circular cross section for different number of cycles. In red colour, the fatigue damage value $D = 1$ is shown, starting from where the failure is considered to start. Up to 200,000 cycles, maximum values of $D = 0.65$ have been reached. However, for 300,000 cycles fatigue damage ($D > 1$) starts in some small areas of the perimeter, although in most parts of the section there are values around 0.7 and 0.8, close to 1. For values of 400,000 cycles, it is observed that almost 50% of the perimeter presents values of fatigue damage $D > 1$, and other areas with values close to 0.6. For this level of fatigue damage, collapse of the bell should already have occurred. Based on the results of this theoretical model, fatigue failure can be expected to occur between 300,000 and 400,000 cycles.

6. Comparison with fatigue failure based on s-n curves for elements under rotational bending loads

In this section, numerical results obtained by FEM have been compared with values and results obtained following a classical approach based on S-N curves, also known as Wöhler curve [24]. The procedure shown in this section presents the solution for fatigue strength of an element under rotational bending loads.

In order to study a fatigue failure, classical approach for design under long cycle fatigue loadings is based on information from SN curves (also known as Wöhler curves [24]), that give conservative predictions about the fatigue behaviour.

From the static and strength points of view the gudgeon can be considered as a beam supported on the bearings at two points, submitted to a central load consisting of the bell, counterweight, braces and clapper equivalent to 28.5 kN. Assuming a simplified model, the stresses that appear at the circular-to-square transition section are those of a bending moment of 1.5 kN·m and a shear of 13.9 kN. Using the typical strength of the materials laws, the von Mises stress amplitude applied in this critical section of the gudgeon due to bending and shear was estimated to be around 92.6 MPa, a value lower than the strength estimated from tensile test and metallurgic analysis, which was 735.7 MPa. This value has been considered on average from hardness and tensile tests.

However, as the bell was swinging at an approximate rate of 35 rpm there was a cyclical inversion of tension–compression loading caused by the variation of positive–negative bending generating inertial forces H, V (Fig. 11) that were transmitted directly to the gudgeon, which in turn transmitted them to the tower through the bearings (Fig. 11). The value of these inertial forces depended on the position of the bell's centre of gravity and its rpm. [4] calculated these results adopting maximum values of dynamic amplification of 1.5 for the vertical and 0.4 for the horizontal load, both referring to the bell's self-weight. Taking this into account, the von Mises stress amplitude applied to this critical section due to bending and shear dynamically amplified by the swinging bell was estimated to be around 139 MPa.

From the bell-ringing program published every year in [3], *El Jaume* bell participated in the chimes approximately 30 times a year at 35 rpm under normal conditions [26], so that it can be estimated that from its restoration in 1992 until it collapsed in 2014 the bell turned round its axis about 346,500 times.

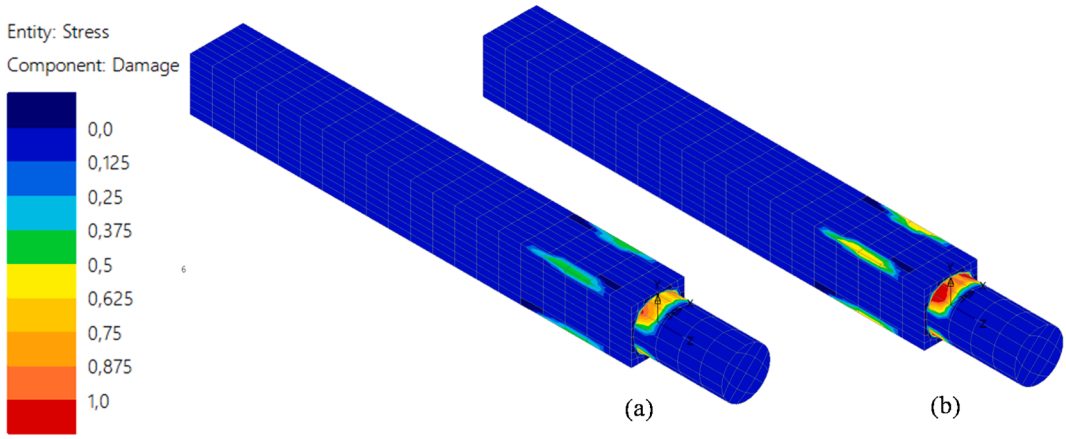

Fig. 9. Fatigue damage in steel axis. (a)- For 300,000 cycles. (b)- for 400,000 cycles.

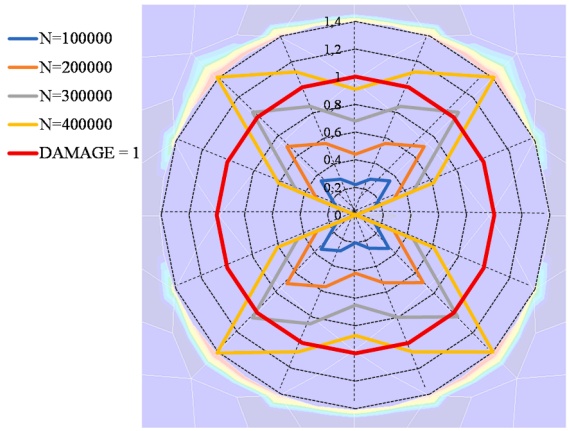

Fig. 10. Fatigue damage propagation in cross section for different number of cycles.

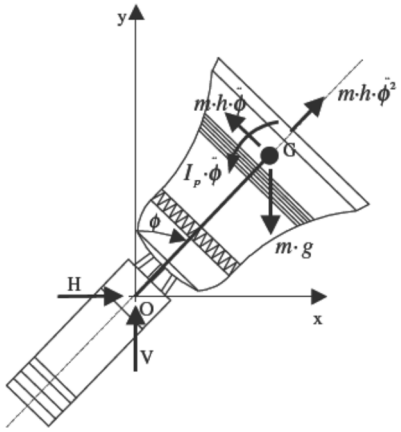

Fig. 11. Simplified bell model obtained from [4].

In order to study a fatigue failure, classical approach for design under long cycle fatigue loadings is based on information from SN curves (also known as Wöhler curves [24]), that give conservative predictions about the fatigue behaviour. These curves vary according to the type of material and the forces involved and are linear when represented on a logarithmic scale. The points that define the straight line are those of the fatigue strength for 10^3 and 10^6 cycles.

On the basis of a large amount of experimental data on steel elements, it can be concluded that the fatigue strength for 10^3 cycles is 0.9 S_u for specimens under rotational bending loads with strength $S_n = 0.5\ S_u$ after 10^6 cycles, where S_u is the material's ultimate strength [41]. If the element is under alternative bending, only the external fibres – furthest from the axis – on the upper and lower surface of the specimen will be subjected to extreme loads. However, if the element is under rotational bending all the exterior fibres will pass successively through the positions of maximum and minimum tension. The fatigue strength of an element under rotational bending loads is thus slightly lower to that of the same element under alternative bending.

The strength is also affected by factors that take into account the effect of surface finish, size, type of load, temperature and stress-concentrating effect. This strength, known as $S_n{}^{Á}$, or fatigue stress can be obtained from Eqs. (3), (4) and (5) [24]:

$$S_n{}^{Á} = K_a \bullet K_b \cdot K_c \cdot K_d \cdot K_e \cdot \left(\frac{S_n}{K_f}\right) \tag{3}$$

$$K_f = 1 + (K_t - 1) \bullet q$$

$$K_t = A\left(\frac{r}{d}\right)^b \tag{5}$$

where:

- $S_n{}^{Á}$ is fatigue stress.
- K_a is coefficient of surface roughness

- K_b is coefficient of size effect.
- K_c is coefficient of load type.
- K_d is coefficient of temperature.
- K_e is coefficient of reliability.
- S_n is theoretical strength after 10^6 cycles, $S_n = 0.5 \bullet S_u$
- K_f is stress concentration coefficient. After the first 1000 cycles, defined by Eq. (4).
- K_t is the theoretical elastic factor, defined by Eq. (5).
- q is notch sensitivity.
- A and b are coefficients obtained from Fig. 8 [24,41].
- r is the transition radius in the stress concentration section.
- d is the diameter of the gudgeon in the axis of the failure section.
- D is the equivalent diameter of the circular section of the widest section of the gudgeon.

7. Discussion of coefficients

The coefficient of surface roughness K_a is defined to consider small imperfections that represent the points most vulnerable to

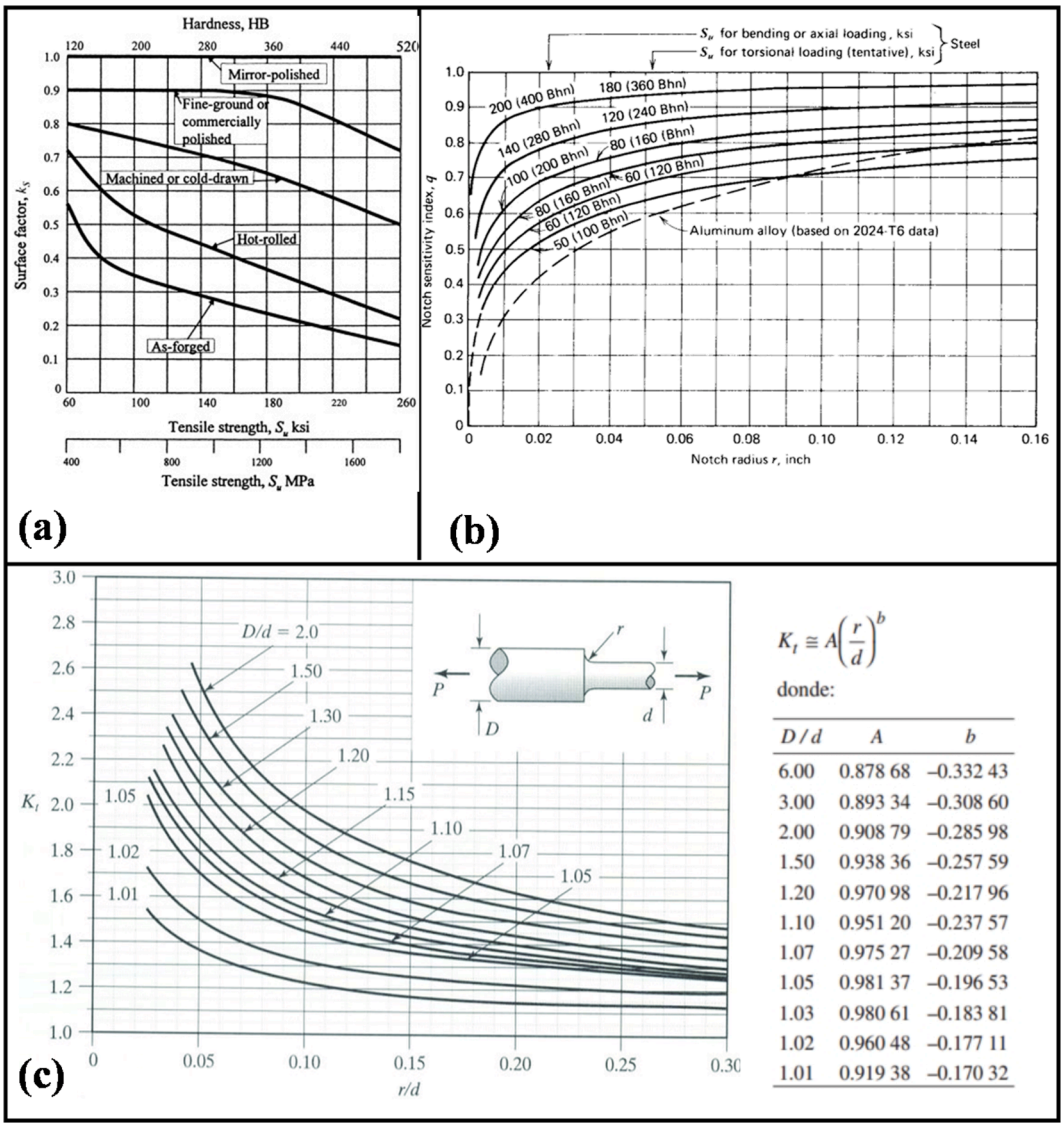

$$K_t \equiv A\left(\frac{r}{d}\right)^b$$

donde:

D/d	A	b
6.00	0.878 68	−0.332 43
3.00	0.893 34	−0.308 60
2.00	0.908 79	−0.285 98
1.50	0.938 36	−0.257 59
1.20	0.970 98	−0.217 96
1.10	0.951 20	−0.237 57
1.07	0.975 27	−0.209 58
1.05	0.981 37	−0.196 53
1.03	0.980 61	−0.183 81
1.02	0.960 48	−0.177 11
1.01	0.919 38	−0.170 32

Fig. 12. Sensitivity factors to obtain fatigue stress. (a) Surface factors for various finishes on steel. [41,43] (b) Fatigue notch sensitivity curves for bending and axial loads, torsion [41,42] (c) Evaluation of the stress concentrator coefficient on a shaft subjected to bending [24].

fatigue crack initiation. Referring to the results published in [24,41], the surface roughness factor of 0.9 (Fig. 12a) can be obtained.

The coefficient of size effect K_b had a value of 0.9 in elements subjected to bending with a diameter larger than 10 mm [24,41]. The type of load coefficient, K_c, adopts a value of 1 as being a bending load [24,41]. The temperature coefficient K_d takes a value of 1, as the temperature was below 450 °C on the day of the failure. The reliability coefficient, K_e is also 1, since the failure had already happened. Table 4 gives a summary of the parameters adopted.

The notch coefficient of ductile steel takes a value of 1 for the stress value at 1000 cycles [24,41]. After 10^6 cycles this value estimated by Eqs. (4) and (5) using the curves in Fig. 12b and c [24,41]. The value of K_f is strongly influenced by the transition radius in the stress concentration section. The evolution of the stress concentration coefficient K_f as a function of the transition radius for the purpose of this study is given in Fig. 13. For quite small values –of the order of 0.01 mm - coefficient K_f reaches values around 4.7. After r values of around 30 mm the concentration factor is reduced to 1 and this notch effect disappears.

The fatigue stress $S_n^{\hat{A}}$ is obtained from a study of the effect of the transition radius. Fig. 14 shows the Stress S - Log (Number of cycles, N) curve, where the curve is considered without the stress concentration effect, the S-N curves considering a stress concentration for a transition radius of 0, 1 and 2.5 mm, and the von Mises stress in the critical shaft section dynamically amplified as indicated in [4].

In view of these results, the fracture of the gudgeon due to the accumulated fatigue damage could have been foreseen in the bell's lifecycle. The main factor for this early fracture depended on the stress concentration effect caused by the abrupt size, transition between both sections. The most unfavourable situation of the break would have been after 355,000 cycles, considering a transition radius of 0 mm, i.e. a 90° joint. If it had been a 1 mm transition the break would have happened around 730,000 cycles. However, the visual inspection showed that there was no transition radius and that the two sections joined at 90°. Considering that the break occurred at 346,500 cycles (from the restoration in 1992 until the collapse in 2014) the failure scenario fits reasonably well with transition radius close to 0. One of the factors that probably could have reduced the bell's service life below the calculated 355,000 cycles and accelerated the fracture was the appearance of oxidation in the crack as shown in Fig. 3. The existence of some indentation marks at the transition zone, caused by the tools used when inserting the gudgeon into the bell wood counterweigths, increased the streses concentration effects and favoured the initiation of multiple cracks, as revealed by the observed ratchet marks in the surface fracture.

It can therefore be concluded that the fracture would not have happened had there been no transition between the gudgeon sections as there would have been no stress concentration effect (Fig. 14). As indicated in Fig. 13, this effect practically disappears after a 30 mm radius, although it could be deduced that the failure would not have occurred had there been a minimum transition radius of 2.5 mm (Fig. 14).

8. Improvements and remedial measures

In view of the final state of the bell and the causes of its failure, it was decided to take different steps as a remedy for the defects detected, consisting of the following measures:

- An immediate stop to ringing all the other bells in the *Micalet* tower, which had been restored in 1992 by the same method as *El Jaume* bell.
- Carry out an inspection of the gudgeon steel shafts of all the bells, consisting of the complete disassembly of the wooden counterweights and gudgeons, followed by non-destructive testing with etching liquids and/or x-rays of the transition sections.
- Replace any gudgeons and counterweights that raised doubts about their fatigue stress reliability.

8.1. Inspection of the gudgeons of the remaining bells.

All the other bells restored in 1992 (*Úrsula, Violant, Barbará, Vicent* and *Andreu*) were completely dismantled by the same technique and procedure as *El Jaume*. Table 5 gives a summary of the initial dimensions of their gudgeons.

The gudgeons of the other bells were a great deal smaller than that of *El Jaume* bell due to having much lighter bell self-weights. However, as all the gudgeons were made by the same technique as *El Jaume* bell, with a section of high stress concentrations that could have shortened their remaining lyfecycle, the decision was made to renew the gudgeons of all the bells as indicated in Table 4.

8.2. Modification of El Jaume's gudgeon dimensions

The gudgeon's dimensions were increased to guarantee its remaining service life. The new gudgeon measures 90x90 mm in the square section and an 80 mm diameter circular section, the hollow in the counterweight was enlarged to 90x90 (Fig. 15a), and larger bearings were installed to accommodate the new 80 mm diameter shafts (Fig. 15b). The new shaft is made of ST52-3 steel according to [42] with a yield strength of 335 MPa and a ultimate strength of between 500 and 630 MPa, suitable for the loads it will be subjected to.

8.3. Modification of circular-to-square transition

This factor had the greatest impact on the gudgeon's fatigue strength deterioration. Fig. 15c shows the solution adopted to modify

Table 4
Parameters adopted to obtain the fatigue stress.

K_a	0.9	A	0.97098
K_b	0.9	b	−0.21796
K_c	1	d (mm)	55
K_d	1	D (mm)	67.7
K_e	1		

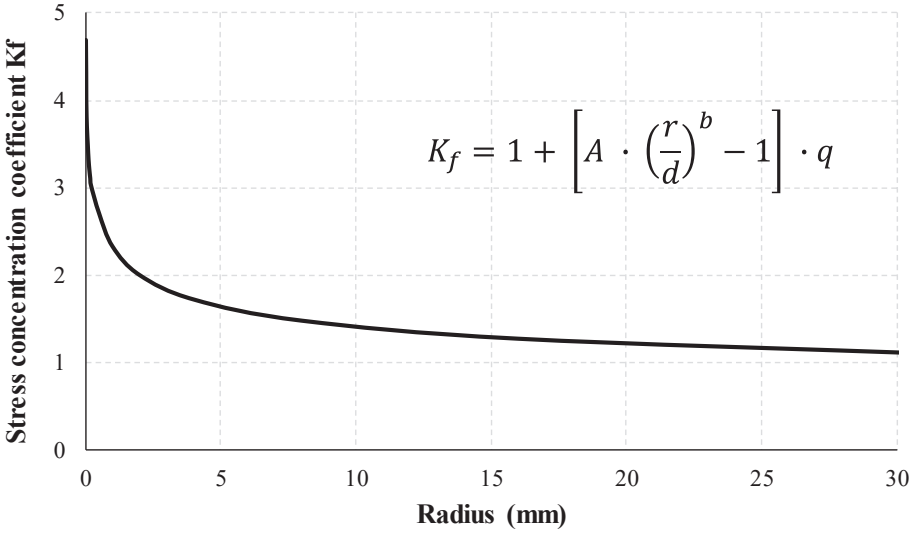

Fig. 13. Evolution of notch coefficient as a function transition radius.

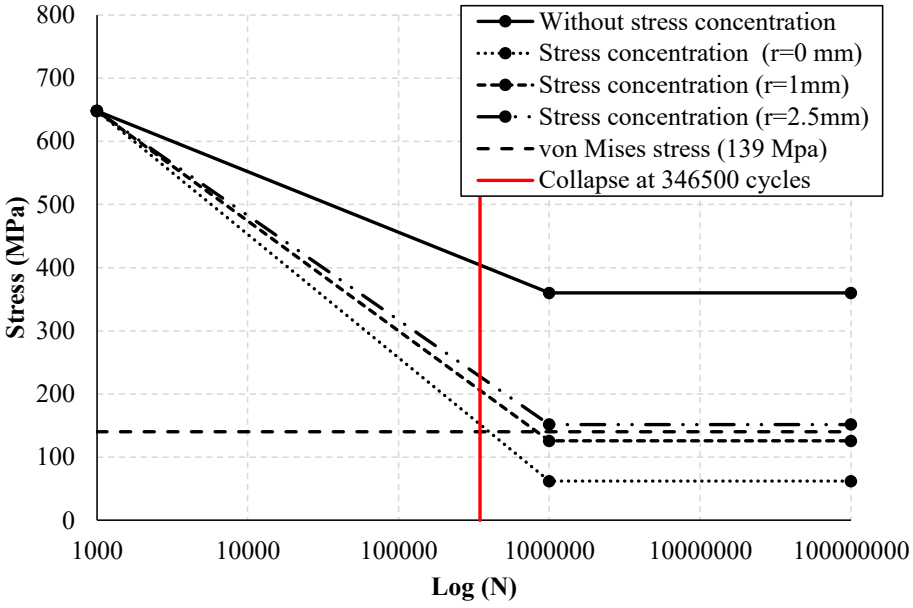

Fig. 14. S-N curves for the broken shaft considering different K_f coefficients.

the union between the circular and square sections to reduce the effect of the stress concentrations and so extend its lyfe service by means of turning the shaft on a lathe. In addition to the increased shaft dimensions, this means the bell is now able to resist the fatigue stresses generated by the swinging.

Table 5

Dimensions of bell gudgeons restored in 1992.[E]

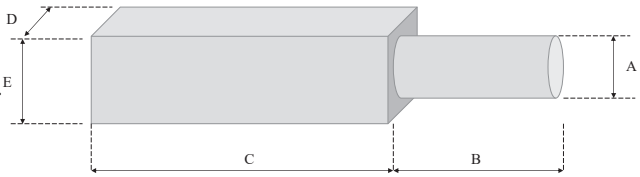

Bell	Bronze weight (kN)	Dimensions (mm)				
		A	B	C	D	E
Úrsula	1.6	35	60	250	40	40
Violant	2.9	35	65	300	40	40
Barbera	3.4	40	100	500	45	45
Vicent	8.3	45	100	550	50	50
Andreu	12.4	45	110	650	50	50
El Jaume	17.5	55	100	600	60	60

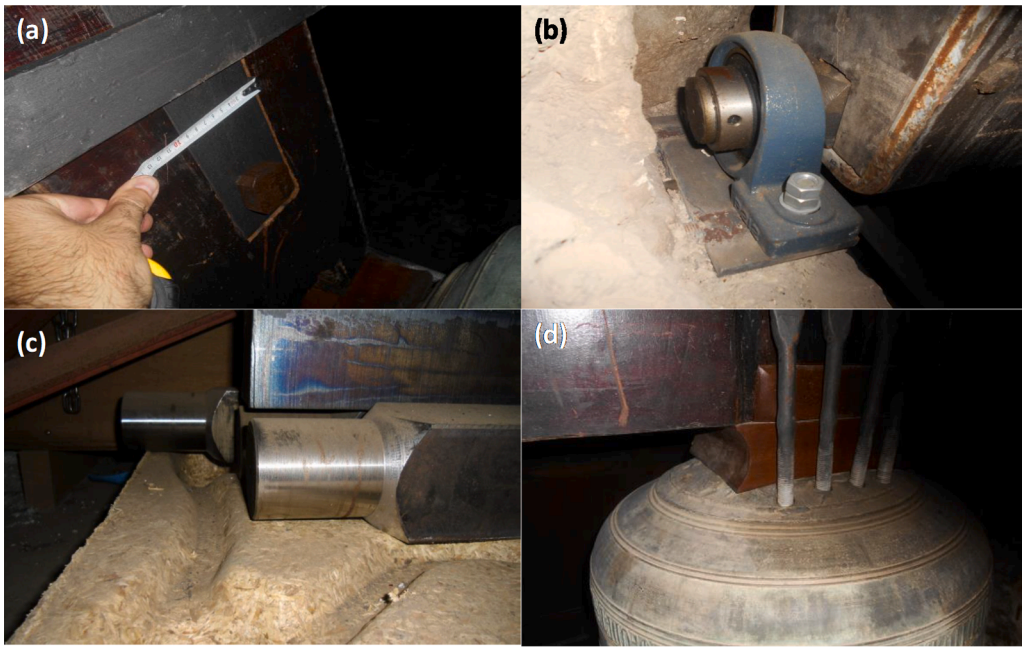

Fig. 15. Remedial measures to *El Jaume*.

8.4. Anchorage of bell to wooden counterweigth

The solutions applied to the canons broken bell to repair the broken *El Jaume* bell are shown in Fig. 15d. These consisted in removing the damaged canons, perforating 8 holes in the bell bronze and connecting them to the upper counterweight by 20 mm diameter circular bars. These were anchored to the interior of the bell by nuts and washers, reinforced the number of connections between the bronze and wood counterweigth and guaranteed the safety against possible failures during swinging.

9. Conclusions

This paper describes and analyses the collapse of the *El Jaume* bell in the Micalet bell tower of Valencia Cathedral when being rung on 25th December 2014, fortunately without casualties.

The visual inspection of the tower and the metallurgical analyses carried out on the bell gudgeon allowed us to focus on the problem. Everything indicated that the collapse occurred due to fatigue failure of the gudgeon due to the cyclical loads generated when the bell was being rung. Following this initial diagnosis, the bell's remaining lifecycle was calculated by means of (1) a fatigue damage numerical model and (2) a S-N curves. From these results it was concluded that after 300,000 cycles, the damage ($D = 1$) began to originate in the perimeter of the circular section. For 400,000 cycles, values of $D > 1$ were reached in more than 50% of the perimeter. Using SN curves, results shows that the bell should have lasted for 355,000 cycles, although the collapse occurred at approximately

346,500 cycles. This reduced fatigue life could have been due to corrosion in the surface of the gudgeon, penetrating inside the crack.

The design of the gudgeon, replaced during the renovation in 1992, was one of the fundamental reasons for the development and propagation of the cracks associated with steel fatigue. This shaft suddenly changed from circular to square without transition, which produced high stress concentrations in the area, considerably reduced the stress fatigue at 10^6 cycles, and made the appearance of not one but several cracks in the surface highly likely.

Another aspect that had a strong influence on the apperance of the cracks was the presence of notches on the surface of the shaft. These irregularities were presumibly caused by the impact of the tools used to insert the gudgeon into the wooden counterweight.

This diagnosis was used to decide on a series of measures designed to avoid the collapse of the remaining bells. These measures consisted of replacing all the gudgeons by others with a gradual transition from square to circular to avoid stresses concentrating in the area that could compromise their remaining lyfe cycle.

The principal lesson learned from this study was the special care that must be taken in elements submitted to bending with cyclic loadings, especially in the section design to avoid a high stress concentration that could cause fatigue failure, especially when these bells are rung manually, since a collapse could have very serious consequences.

It should be noted that the authors do not consider that large bells are especially prone to failure. This depends on the design of the elements subjected to cyclical loading, whose life cycle could be seriously reduced by fatigue damage. It is possible to find examples of historical bells such as the *Emmanuelle* in the Notre Dame Cathedral that have been in service without failures for a considerable time. However, other bells, such as the Freedom Bell in Berlin, the Liberty Bell in Philadelphia, Big Ben in London, St. Peteŕs Bell in Cologne or the case of the *El Jaume* bell cited here, that have given problems and generated uncertainty about possible future collapses.

Declaration of Competing Interest

The authors declare the following financial interests/personal relationships which may be considered as potential competing interests: [Salvador Ivorra reports a relationship with University of Alicante that includes: employment.].

Acknowledgements

Authors would acknowledge to Dr. Francesc Llop and all the team of *Gremi de Campaners de la Catedral de València (The guild of Valencia Cathedral bell ringers)* for their collaboration in this research as well as the companies *2001 Técnica y Artesanía S. L. L.* and *Electro Recamp S.L.* for their support.

References

[1] Royal Decree 296/2019, of April 22, which declares the Manual Ringing of the Bell as a Representative Manifestation of the Intangible Cultural Heritage. Available from: <https://www.boe.es/boe/dias/2019/04/23/pdfs/BOE-A-2019-6064.pdf> (in Spanish).
[2] Luis del Campo, Algunos aspectos del tocar de las campanas, Cuadernos de etnología y etnografía de Navarra, ISSN 0590-1871, Año n° 20, N° 51 (1988) 65–178 (in Spanish).
[3] Gremi de Campaners de la Catedral de Valencia, (2021, 5, 10). Available from: <https://www.campaners.com>.
[4] S. Ivorra, M.J. Palomo, G. Verdú, A. Zasso, Dynamic forces produced by swinging bells, Meccanica 41 (1) (2006) 47–62.
[5] S. Ivorra, F.J. Pallarés, J.M. Adam, Masonry bell towers: dynamic considerations, Proc. Inst. Civil Eng. – Struct. Build. 164 (1) (2011) 3–12.
[6] Adolfo Preciado, Juan Carlos Santos, Citlalli Silva, Alejandro Ramírez-Gaytán, José Manuel Falcon, Seismic damage and retrofitting identification in unreinforced masonry Churches and bell towers by the September 19, 2017 (Mw = 7.1) Puebla-Morelos earthquake, Eng. Failure Anal. 118 (2020) 104924.
[7] E.H. Lewis, Calculation of the Forces Acting upon a Church Tower When Bells are Rung. May 1914. Guildford. GU1 1BL. Library of the Central Council of Chuch Bell Ringers at Penmark House, United Kingdom, 1914.
[8] J. Wilson, A. Selby, Engineering a Cathedral, Thomas Telford Ltd., London, 1993, p. p. 77_100.
[9] A.R. Selby, J.M. Wilson, Dynamic behaviour of masonry church bell towers, in: A.E. Schultz, S.L. McCabe (Ed.), Worldwide Advances in Structural Concrete and Masonry, Proceedings of the CCMS Symposium, ASCE, New York, 1997, p. 188_99.
[10] F.P. Müller, Berechnung und Konstrucktion von Glockentürmen, Whilhelm Ernst &Sohn, Berlin, 1968 [in German].
[11] F.P. Müller, Dynamische und statische Gesichtspunkte beim Bau von Glockentürmen, Badenia Verlag GmbH, Karslsruhe, 1986, p. 201_12 (in German).
[12] Steiner J. Neukonstruktion und Sanierung von Glockentürmen nach statischen und dynamischen Gesichtspunkten, Badenia Verlag GmbH, Karslsruhe, 1986, p. 213_37 (in German).
[13] K.G. Schutz, Dynamische Beanspruchung von Glockentürmen, Bauingenieur 69. Springer-Verlag, 1994, p. 211_7 (in German).
[14] A. Preciado, G. Bartoli, H. Budelmann, Fundamental aspects on the seismic vulnerability of ancient masonry towers and retrofitting techniques, Earthquakes Struct. 9 (2) (2015) 339–352.
[15] A. Preciado, H. Budelmann, G. Bartoli, Earthquake protection of colonial bell towers in Colima, Mexico with externally prestressed FRPs, Int. J. Archit. Heritage 10 (4) (2016) 499–515.
[16] S. Ivorra, F. Pallarés, J.M. Adam, Dynamic behavior of a modern bell tower – a case study, Eng. Struct. 31 (2009) 1085_1092.
[17] Z. Zhu, Y. Zhu, Q. Wang, Fatigue mechanisms of Wheel rim Steel under off-axis loading, Mater. Sci. Eng., A 773 (2020), 138731.
[18] A. Cavuto, M. Martarelli, G. Pandarese, G.M. Revel, E.P. Tomasini, Train wheel diagnostics by laser ultrasonics, Measurement 80 (2016) 99–107.
[19] Y. Li, V. Aubin, C. Rey, P. Bompard, Microstructural modelling of fatigue crack initiation in austenitic steel 304L, Proc. Eng. 31 (2012) 541–549.
[20] R. Pérez-Mora, T. Palin-Luc, C. Bathias, P.C. Paris, Very high cycle fatigue of a high strength steel under sea water corrosion: a strong corrosion and mechanical damage coupling, Int. J. Fatigue 74 (2015) 156–165.
[21] D. Bettge, C.-P. Bork, Failures of Berlin Freedom Bell since 1966, Eng. Fail. Anal. 43 (2014) 63–76.
[22] H.J. Petroski, On the cracked Bell, J. Sound Vib. 96 (4) (1984) 485–493.
[23] A. Orlando, L. Pagnini, M.P. Repetto, Structural response and fatigue assessment of a small vertical axis wind turbine under stationary and non-stationary excitation, Renew. Energy 170 (2021) 251–266.
[24] Robert L. Norton, Machine Design, fifth ed. Pearson (Ed.), September 16, 2013.
[25] Francesc Llop i Álvaro, Las campanas de la Catedral de València, Universitat de València, Facultat de Geografía i Història, 2011. Available from: <http://campaners.com/php/textos.php?text=824> (in Spanish).
[26] Francisco Mas Gadea, Toques de la Catedral de Valencia, 1989, Available from: <http://campaners.com/php/textos.php?text=1536#2.6> (in Spanish).

[27] Decree 217/2018, of November 30, of the Consell, which declares movable property of cultural interest, the set of 70 Gothic bells of the Valencian Community. Available from: <https://www.boe.es/boe/dias/2019/01/18/pdfs/BOE-A-2019-610.pdf> (in Spanish).
[28] Salvador Ivorra, Acciones dinámicas introducidas por las vibraciones de las campanas sobre torres-campanario, Universitat Politècnica de València, PhD, 2002.
[29] S. Ivorra, F. Llop, Determinación de algunas características físicas de una campana. [Determination of some physical characteristics of a bell.] Congreso de Conservación y Restauración de Bienes Culturales, vol. 2. Secretaría Técnica del Congreso, Valladolid, 2002, pp. 891–900 (in Spanish).
[30] Metals Handbook, American Society for Metals, Metals Park, Ohio, vol. 10, 8a, Ed. 1975, p. 102.
[31] S. Seifoori, A.M. Parrany, M. Khodayari, A high-cycle fatigue failure analysis for the turbocharger shaft of BELAZ 75131 mining dump truck, Eng. Fail. Anal. 116 (2020), 104752.
[32] E. Santos, J. Yenque, O. Rojas, V. Rosales. Notas científicas acerca del ensayo de dureza, Ind. Data 4 (2) (2001) 73–80 (in Spanish).
[33] ISO 6892-1:2019, Metallic materials - Tensile testing - Part 1: Method of test at room temperature.
[34] ISO 377:2017, Steel and steel products - Location and preparation of samples and test pieces for mechanical testing.
[35] ISO 18265:2013, Metallic materials - Conversion of hardness values.
[36] ISO 683-1:2016, Heat-treatable steels, alloy steels and free-cutting steels - Part 1: Non-alloy steels for quenching and tempering.
[37] ISO 643:2019, (Corrected version 2020-03). Steels - Micrographic determination of the apparent grain size.
[38] UNE-EN 10083-2: 2008, Steels for quenching and tempering - Part 2: Technical delivery conditions for non-alloy steels.
[39] Lusas, Lusas Reference Manual, Surrey (UK), 2010.
[40] M. Ciavarella, P.Ď. Antuono, G.P. Demelio, A simple finding on variable amplitude (Gassner) fatigue SN curves obtained using Mineŕs rule for unnotched or notched specimen, Eng. Fract. Mech. 176 (2017) 178–185.
[41] Ansel C. Ugural, Mechanical Design of Machine Components: SI Version, 2018.
[42] R.C. Juvinall, Engineering Consideration of Stress, Strain, and Strength, McGraw-Hill, New York, 1967.
[43] G. Sines, J.L. Waisman (Eds.), Metal Fatigue, McGraw-Hill, New York, 1959.